JOURNAL OF COMPUTATIONAL PHYSICS 49, 44–66 (1983)

Computational Studies of First-Born Scattering Cross Sections I. Spectral Properties of Bethe Surfaces

D. J. MARGOLIASH*

Department of Chemistry, Indiana University, Bloomington, Indiana 47405

AND

P. W. LANGHOFF†

Laboratoire des Collisions Atomiques et Moléculaires, Université Paris-Sud, 91405 Orsay Cedex, France

Received January 21, 1982

Computational techniques are reported for studies of atomic and molecular first-Born inelastic charged-particle scattering cross sections. Detailed illustrative results are presented for hydrogenic targets of appropriately defined momentum-transfer-dependent spectral moments, scattering cross sections differential in momentum transfer and in scattering angle, total inelastic scattering cross sections as functions of incident energy, and Van Hove autocorrelation functions describing target charge-density fluctuations. The variations with momentum transfer of the moments, the origins of the structures and asymptotic behaviors of the correlation functions, and the general characteristics of the scattering cross sections are described and clarified on the basis of the shape of the corresponding Bethe surface. Evaluations of the Born scattering cross sections differential in angle and in momentum transfer help to clarify the ranges of validity of various forms of corresponding static and binary-encounter approximations. The Bethe–Inokuti sum rule for the total inelastic scattering cross section is recovered in a transparent fashion from the static approximation by taking an appropriate high-energy limit, and its range of validity, as well as those of the static and binary-encounter approximations, is clarified by comparison with the correct Born result. Careful treatments of the scattering kinematics are seen to be important in these connections. It is noted throughout that spectral moments of the Bethe surface provide sufficient information for evaluation of Born cross sections, the consequences of which are investigated in a companion article in this issue.

I. INTRODUCTION

Fast charged particles generally straggle and stop in condensed matter, losing energy by electronic excitation or ionization of the target's atomic or molecular

* Present address: Department of Chemistry, University of Western Ontario, London, Ontario, Canada N6A 5B7.

† Permanent address: Department of Chemistry, Indiana University, Bloomington, Indiana 47405.

0021-9991/83/010044-23$03.00/0

constituents [1–3]. By contrast, single scattering events can be made to dominate in sufficiently low density gases, providing measurements of cross sections differential in angle and energy loss useful for elucidating the electronic excitation spectra of individual atoms and molecules [4–6]. Although theoretical expressions for the appropriate high-energy inelastic scattering and excitation cross sections [7–10], and for the mean energies of straggling, excitation, and stopping [1–3] are well known—dating from the early work of Bethe [11]—detailed computational applications of the theory are generally limited by difficulties that arise in constructing appropriate complete sets of atomic or molecular eigenfunctions and associated discrete and continuum generalized oscillator strengths [12]. Moreover, even when the complete Bethe surface of discrete and continuum generalized oscillator strengths is available, troublesome one- and two-dimensional quadratures at constant scattering angle or momentum transfer must be evaluated to determine the relevant cross sections. Consequently, so-called static, binary-encounter, and sum-rule or closure approximations to the differential and total inelastic scattering cross sections are generally employed in lieu of the correct Born results [4–10]. In view of the continuing interest in charged-particle energy loss in condensed matter and in electron impact-excitation spectroscopy, it would seem useful to devise convenient techniques for constructing Bethe surfaces and associated Born scattering cross sections that can be applied to complex atomic and molecular targets, and to carify aspects of presently employed computational approximations.

In the present article, spectral properties of Bethe surfaces are studied to establish a basis for the formulation of alternatives to the conventional computational approach, and to clarify the ranges of validity of static, binary-encounter, and sum-rule approximations to Born differential and total inelastic scattering cross sections. Detailed computations are reported for hydrogenic targets of negative-integer spectral power moments that are momentum-transfer dependent [13], scattering cross sections differential in momentum transfer and in scattering angle [4–6], total inelastic scattering cross sections as functions of incident electron energy [7–10], and so-called Van Hove autocorrelation functions describing target charge-density fluctuations [14]. Careful quadrature and summation techniques are seen to be required for precise evaluations of these spectral properties, which are somewhat scattered in the literature or have gone previously unreported.

The discrete and continuum portions of the calculated spectral moments are seen to vary with momentum transfer in accordance with the shape of the corresponding Bethe surface. Conversely, it is indicated that moments define optimal generalized Gaussian quadratures for evaluations of spectral-integral properties. The ranges of validity of static and binary-encounter approximations [4–6] to scattering cross sections differential in scattering angle and in momentum transfer are clarified fully by comparisons with the corresponding correct Born results. Similarly, the range of validity of the Bethe–Inokuti sum rule [8] for the total inelastic scattering cross section is determined by comparison with the Born result evaluated using two-dimensional quadratures, and its connection with the high-energy limits of static and binary-encounter approximations is clarified. Proper treatments of the limiting forms

of the scattering kinematics are seen to be essential in these connections. Finally, it is indicated that Van Hove autocorrelation functions can provide an alternative computational approach to determinations of Bethe surfaces and corresponding Born scattering cross sections [8], an approach that has yet to be adopted fully in the literature.

In Section II, the Bethe–Born theory of inelastic scattering is described briefly in order to establish notational conventions, and the generalized oscillator-strength distribution, or Bethe surface, is identified. The various spectral properties studied here are defined in Section III, and their evaluations reported and discussed in Section IV. Some general and concluding remarks are made in Section V. Certain of the suggestions made and conclusions drawn in the present report are pursued in a companion article in this issue.

II. The Bethe–Born Approximation

The inelastic cross section differential in excitation energy and momentum transfer for the scattering of fast electrons from an individual atomic target, assumed for simplicity to have an infinite nuclear mass, can be written in the Bethe–Born approximation (Hartree atomic units are employed unless indicated otherwise) as [4–10, 15]

$$d^{(2)}\sigma(\varepsilon, q) = (2\pi/qt\varepsilon)\, df(\varepsilon, q)\, dq\, \delta(t - \varepsilon - k_2^2/2). \tag{1}$$

Here, t is the incident electron kinetic energy, ε is the atomic excitation energy, and $q = |\mathbf{k}_1 - \mathbf{k}_2|$ is the magnitude of the momentum transferred to the atomic target, with $\mathbf{k}_2$ and $\mathbf{k}_1$ the final and initial momenta of the scattered electron, respectively. The generalized oscillator strength $df(\varepsilon, q)$ for atomic excitation into the energy interval ε to $\varepsilon + d\varepsilon$ upon transfer of momentum q to the atomic target can be written

$$df(\varepsilon, q) = \left[\sum_{n=1}^{\infty} f_n(q)\, \delta(\varepsilon_n - \varepsilon) + g(\varepsilon, q) \right] d\varepsilon, \tag{2}$$

where

$$f_n(q) = \sum_{\Gamma} 2\varepsilon_n \left| \langle \phi_{n,\Gamma} | (1/q) \exp(i\mathbf{q} \cdot \mathbf{r}) | \phi_0 \rangle \right|^2 \tag{3a}$$

and

$$g(\varepsilon, q) = \sum_{\Gamma} 2\varepsilon \left| \langle \phi_{\varepsilon,\Gamma} | (1/q) \exp(i\mathbf{q} \cdot \mathbf{r}) | \phi_0 \rangle \right|^2 \tag{3b}$$

are the discrete generalized oscillator strengths and continuum generalized oscillator-strength density, respectively, which comprise the so-called Bethe surface [7–11]. Equations (2) and (3) are written arbitrarily for a one-electron atomic target with

nondegenerate ground state ϕ_0, although most of the development is not limited to this case. The discrete excitation energies ε_n and eigenfunctions $\phi_{n,\Gamma}$ have their customary meanings, the form of Eq. (3b) implies the continuum eigenfunctions $\phi_{\varepsilon,\Gamma}$ are delta-function normalized in the excitation energy [16], and the summations in Eqs. (3) are over all quantum numbers Γ labelling degeneracy. The energy-conserving delta function is included in Eq. (1) to emphasize that the variables q and ε are not entirely independent, and must satisfy the kinematic relation

$$q^2 = 4t(1 - (\varepsilon/2t) - (1 - \varepsilon/t)^{1/2} \cos\theta), \tag{4}$$

where θ is the scattering angle between $\mathbf{k}_1$ and $\mathbf{k}_2$. In spite of the kinematical constraint of Eq. (4), which follows from the definition of q and conservation of energy, it is customary and convenient when referring to the generalized oscillator strength $df(\varepsilon, q)$ of Eqs. (2) and (3) to consider its behavior for all ε and q.

As noted originally by Bethe [11], and in a somewhat more general context by Van Hove [14], the particularly simple form taken by Eq. (1) is, in part, a consequence of employing q and ε rather than θ and ε as variables. In the present development, q and ε are generally preferred, although the kinematic relation of Eq. (4) can always be employed to replace the momentum transfer q with the appropriate scattering angle θ at a given excitation energy ε. In this case, the doubly differential inelastic scattering cross section takes the form

$$d^{(2)}\sigma(\varepsilon, \theta) = (4\pi/\varepsilon q(\varepsilon, \theta)^2)(1 - \varepsilon/t)^{1/2}\, df(\varepsilon, q(\varepsilon, \theta)) \sin\theta\, d\theta, \tag{5}$$

where the dependence of momentum transfer $q(\varepsilon, \theta)$ (Eq. (4)) on scattering angle θ and excitation energy ε is explicitly indicated, making the energy-conserving delta function of Eq. (1) unnecessary in Eq. (5). The factor $(1 - \varepsilon/t)^{1/2}$ appearing in Eqs. (4) and (5) is seen to be the ratio of the magnitudes of final to initial momentum k_2/k_1 of the scattered electron.

III. Spectral Properties of Bethe Surfaces

The spectral properties of Bethe surfaces of interest here, which can be expressed as Riemann–Stieltjes integrals over the appropriate generalized oscillator-strength distributions, are defined in this section.

A. Spectral Moments

Equations (3) can be employed in determining the Bethe surface [Eq. (2)] for a particular target when the necessary eigenstates $\phi_{n,\Gamma}$ and $\phi_{\varepsilon,\Gamma}$ are available in convenient forms. More generally, it is useful to recognize that

$$df(\varepsilon, q) \geqslant 0, \qquad \varepsilon_1 \leqslant \varepsilon < \infty \tag{6}$$

for fixed momentum transfer q or scattering angle θ and an atomic target in its

ground state. Consequently, the cumulative generalized oscillator-strength distribution

$$f(\varepsilon, q) = \int_{\varepsilon_1}^{\varepsilon} df(\varepsilon', q) = \int_{\varepsilon_1}^{\varepsilon} \left[\sum_{n=1}^{\infty} f_n(q)\, \delta(\varepsilon_n - \varepsilon') + g(\varepsilon', q) \right] d\varepsilon' \tag{7}$$

is a nondecreasing function of ε for fixed q or θ. Such distributions are characterized uniquely by their power moments [17, 18], which in the case of fixed momentum transfer q are written in the form [13]

$$S(q, i) = \int_{\varepsilon_1}^{\infty} \varepsilon^i\, df(\varepsilon, q), \qquad i \leqslant 2. \tag{8}$$

Alternatively, spectral moments corresponding to fixed scattering angle θ can also be defined, although these are not employed explicitly here.

A finite number of spectral moments define a set of optimal generalized Gaussian quadratures useful for evaluating integral properties of the Bethe surface, and for the construction of the corresponding distribution $f(\varepsilon, q)$ [17–19]. Consequently, it is important to study the moments of Eq. (8), and to note that they can be computed without reference to the eigenstates $\phi_{n,\Gamma}$ and $\phi_{\varepsilon,\Gamma}$. Enforcing closure in Eq. (8) gives

$$S(q, i) = 2\langle \phi_0 | (1/q) \exp(-i\mathbf{q} \cdot \mathbf{r})(H_0 - E_0)^{i+1} (1/q) \exp(i\mathbf{q} \cdot \mathbf{r}) | \phi_0 \rangle, \tag{9}$$

where Eqs. (2) and (3) have been employed, and $(H_0 - E_0)^{i+1}$ is defined in the subspace orthogonal to ϕ_0. In the cases $i = 2, 1, 0$, and -1, Eq. (9) provides expressions for $S(q, i)$ as expectations values over the ground-state wavefunction [20]. For $i < -1$, Eq. (9) can be evaluated employing complete sets of L^2 basis functions [19], or appropriate integral-transform techniques in certain cases [21], without prior construction of the $\phi_{n,\Gamma}$ and $\phi_{\varepsilon,\Gamma}$.

B. Scattering Cross Sections

Although experiments are generally performed at a fixed scattering angle, it is convenient for computational purposes to consider the inelastic cross section differential in momentum transfer. This quantity is obtained from Eq. (1) by integration over excitation energy in the form

$$d^{(1)}\sigma(q) = (2\pi/qt)\, S(\varepsilon_{\max}(q), q)\, dq, \tag{10a}$$

where

$$S(\varepsilon_{\max}(q), q) = \int_{\varepsilon_1}^{\varepsilon_{\max}(q)} (1/\varepsilon)\, df(\varepsilon, q) \tag{10b}$$

and

$$\varepsilon_{\max}(q) = q(2t)^{1/2} - q^2/2 \tag{10c}$$

is the maximum allowable excitation energy at a given allowable momentum transfer

q, determined from Eq. (4) with θ equal to 0 or π for q less than or greater than $(2t)^{1/2}$, respectively. The energy-conserving delta function in Eq. (1) limits the integration in Eq. (10b) to the indicated range. In addition, as the integration proceeds from ε_1 to $\varepsilon_{max}(q)$ at fixed momentum transfer q, the kinematic relation of Eq. (4) requires that the scattering angle vary between its extreme values $\theta_{max}(q)$ and $\theta_{min}(q)$. These are conveniently tabulated in the forms

$$\theta_{min}(q) = 0, \qquad \theta_{max}(q) = \theta(q, \varepsilon_1); \qquad q_{min} \leqslant q \leqslant (2\varepsilon_1)^{1/2}, \tag{11a}$$

$$\theta_{min}(q) = 0, \qquad \theta_{max}(q) = \sin^{-1}[q/(2t)^{1/2}]; \qquad (2\varepsilon_1)^{1/2} \leqslant q < (2t)^{1/2}, \tag{11b}$$

$$\theta_{min}(q) = \theta(q, \varepsilon_1), \qquad \theta_{max}(q) = \pi/2; \qquad q = (2t)^{1/2}, \tag{11c}$$

$$\theta_{min}(q) = \theta(q, \varepsilon_1), \qquad \theta_{max}(q) = \pi; \qquad (2t)^{1/2} < q \leqslant q_{max}. \tag{11d}$$

Here, $\theta(q, \varepsilon_1)$ is obtained by solving Eq. (4) for θ with $\varepsilon = \varepsilon_1$, and $q_{min/max}$ is the smallest/largest overall allowable momentum transfer for given indicent energy t (Eq. (14b)). Consequently, the cross section differential in momentum transfer (Eqs. (10)) does not correspond to a single scattering angle, but, rather, to the range of angles $\theta_{min}(q)$ to $\theta_{max}(q)$ for a given value q of momentum transfer, indicated by Eqs. (11). Although the cross section of Eqs. (10) is generally not directly measurable, it can be constructed from experimental data by appropriate kinematical analysis, and, moreover, provides a convenient vehicle for clarifying static and sum-rule approximations to total inelastic scattering cross sections.

The inelastic cross section differential in scattering angle, which can be measured more directly than the cross section of Eqs. (10), is obtained from Eq. (5) by integrating over excitation energy in the form

$$d^{(1)}\sigma(\theta) = 4\pi F(\theta) \sin\theta \, d\theta, \tag{12a}$$

where

$$F(\theta) = \int_{\varepsilon_1}^{t} ((1 - \varepsilon/t)^{1/2}/\varepsilon q(\varepsilon, \theta)^2) \, df(\varepsilon, q(\varepsilon, \theta)). \tag{12b}$$

Generally, Eq. (12a) does not correspond to a single value of momentum transfer, since $q(\varepsilon, \theta)$ varies over its kinematically allowable range (Eq. (4)) as the integration in Eq. (12b) proceeds from ε_1 to t. The extreme values of momentum transfer are obtained from Eq. (4) at fixed angle θ in the forms

$$q_{min}(\theta) = q(\varepsilon_1, \theta), \qquad \text{for} \quad 0 \leqslant \theta \leqslant \theta_1, \tag{13a}$$

$$= (2t)^{1/2} \sin\theta, \qquad \text{for} \quad \theta_1 \leqslant \theta \leqslant \pi/2, \tag{13b}$$

$$= (2t)^{1/2}, \qquad \text{for} \quad \pi/2 \leqslant \theta \leqslant \pi, \tag{13c}$$

$$q_{max}(\theta) = (2t)^{1/2}, \qquad \text{for} \quad 0 \leqslant \theta \leqslant \theta_2, \tag{13d}$$

$$= q(\varepsilon_1, \theta), \qquad \text{for} \quad \theta_2 \leqslant \theta \leqslant \pi, \tag{13e}$$

where

$$\theta_1 = \cos^{-1}[(1-\varepsilon_1/t)^{1/2}] \cong 0, \tag{13f}$$

$$\theta_2 = \cos^{-1}[\tfrac{1}{2}(1-\varepsilon_1/t)^{1/2}] \cong \pi/3, \tag{13g}$$

and $q(\varepsilon_1, \theta)$ is given by Eq. (4) with $\varepsilon = \varepsilon_1$.

The kinematical limits of Eqs. (11) and (13) are written out in detail to emphasize that the singly differential cross sections of Eqs. (10) and (12) refer to different paths of integration over the Bethe surface in the $\varepsilon - q$ plane. Consequently, different portions of the Bethe surface generally control the values of the cross sections of Eqs. (10) and (12), and different approximations are appropriate in computational studies. In addition to the two latter singly-differential cross sections, the inelastic cross section differential in excitation energy is obtained by integrating Eq. (1) over all kinematically allowed momentum transfer at fixed ε, or by integrating Eq. (5) over all scattering angles at fixed ε [8], although this quantity is not considered explicitly here.

The total inelastic scattering cross section at incident energy t is obtained from Eq. (10) by integrating over all momentum transfer in the form [4–10]

$$\sigma_{\text{inelastic}} = (2\pi/t)\int_{q_{\min}}^{q_{\max}} (1/q)\, S(\varepsilon_{\max}(q), q)\, dq, \tag{14a}$$

where

$$q_{\max/\min} = (2t)^{1/2} \pm (2t - 2\varepsilon_1)^{1/2} \cong [2(2t)^{1/2}]/[\varepsilon_1/(2t)^{1/2}] \tag{14b}$$

is the largest/smallest allowable momentum transfer, obtained from Eq. (4) with $\theta = \pi/0$ and $\varepsilon = \varepsilon_1$. Note that $q_{\min} \cong 0$ and $q_{\max}$ is approximately twice the momentum of the incident electron. An alternative expression for the total inelastic scattering cross section which is formally identical to Eq. (14a) is obtained by integrating Eq. (12a) over all scattering angles in the form

$$\sigma_{\text{inelastic}} = 4\pi \int_0^{\pi} F(\theta) \sin\theta\, d\theta. \tag{15}$$

The development of Eqs. (10)–(15) emphasizes that the Bethe surface (Eqs. (2) and (3)) provides the dynamical information required to construct high-energy inelastic electron-scattering cross sections. It is clear, however, that even with explicit analytical expressions for $df(\varepsilon, q)$, the necessary quadratures, particularly those of Eqs. (14) and (15) requiring double integration, can be troublesome. Moreover, more generally the necessary Bethe surface is unavailable, and appropriate computational approximations are required for construction of scattering cross sections.

C. *Van Hove Autocorrelation Functions*

Although the Bethe surface of Eqs. (2) and (3) specifies the inelastic process of

interest here, it is convenient and helpful to consider also the corresponding autocorrelation function for scattering. The Fourier integral transform

$$\Phi(q, t) = (q^2/2) \int_{\varepsilon_1}^{\infty} (1/\varepsilon)\, e^{i\varepsilon t}\, df(\varepsilon, q) \tag{16a}$$

of the generalized oscillator-strength distribution defines the appropriate Van Hove function [14]. Using Eqs. (2) and (3), $\Phi(q, t)$ can be written in the alternative form

$$\Phi(q, t) = \langle \phi_0 \,|\mu(\mathbf{q}, 0)\, \mu(\mathbf{q}, t)|\, \phi_0 \rangle - |\langle \phi_0 \,|\mu(\mathbf{q}, 0)|\, \phi_0 \rangle|^2, \tag{16b}$$

where

$$\mu(\mathbf{q}, t) = e^{i\mathbf{q}\cdot\mathbf{r}(t)} \tag{17a}$$

and

$$\mathbf{r}(t) = e^{iH_0 t}\, \mathbf{r}\, e^{-iH_0 t} \tag{17b}$$

is the position operator of the target electron in the interaction picture. Equation (16b) evidently corresponds to a position-time autocorrelation function for target-atom electrons. The use of such so-called intermediate scattering or correlation functions in descriptions of the absorption and scattering of light—and of the scattering of particles—by crystals, liquids, and gases is widespread [22], although applications to electron scattering by individual atoms and molecules have not been previously reported. Subsequent Fourier transformation of Eq. (16b) in the momentum-transfer variable $\mathbf{q}$ to the conjugate position variable $\mathbf{r}$ gives the full space and time Van Hove autocorrelation function for the electrons of the atomic target [14]. It is convenient in the present development, however, to limit attention to density fluctuations associated with a given wave number q, and thus to deal with Eq. (16a). Note that Eq. (16a) refers to Fourier transformation of the inelastic portion of the Born cross section. When the corresponding elastic contribution is included in the Fourier transform an additional time-independent term—proportional to the so-called atomic form factor—appears in the resulting correlation function [14]. This term is explicitly subtracted in Eq. (16b), emphasizing that only inelastic contributions are included in the definition of Eq. (16a).

It is of some interest to note that the conventional moment-expansion approach to time autocorrelation functions is not directly applicable in the present case [22]. That is, introduction of a Taylor series expansion in Eq. (16a) gives

$$\begin{aligned} \Phi(q, t) &= (q^2/2) \int_{\varepsilon_1}^{\infty} (1/\varepsilon) \sum_{k=0}^{\infty} [(i\varepsilon t)^k/k!]\, df(\varepsilon, q) \\ &= (q^2/2) \sum_{k=0}^{\infty} [(it)^k/k!]\, S(q, k-1), \end{aligned} \tag{17c}$$

where the order of integration and summation has been interchanged in the usual

way. Since the moments $S(q, k-1)$ (Eq. (8)) diverge for $k \geqslant 3.5$, it is clear Eq. (16c) is useful only in the limit $t \to 0$. Because the integrand of Eq. (16a) is oscillatory, it is also clear that direct evaluation of the autocorrelation function by quadratures when $df(\varepsilon, q)$ is known can be troublesome, and requires careful treatment.

IV. Calculations in Atomic Hydrogen

Atomic hydrogen provides a useful example for investigating the spectral-integral properties of Bethe surfaces. In this case, the discrete and continuum portions of the generalized oscillator-strength spectra are given by the expressions [7–11]

$$\varepsilon_n = \tfrac{1}{2}[1 - (1/n^2)], \qquad n = 2, 3,..., \tag{18a}$$

$$f_n(q) = \frac{2^8 n^5 (n^2-1)[(n^2-1)/3 + n^2q^2][(n-1)^2 + n^2q^2]^{(n-3)}}{[(n+1)^2 + n^2q^2]^{(n+3)}}, \quad n = 2, 3,..., \tag{18b}$$

$$g(\varepsilon, q) = \frac{2^9 \varepsilon (q^2 + 2\varepsilon/3) \exp[-2k(\varepsilon)^{-1} \tan^{-1}(2k(\varepsilon)/(q^2 - 2\varepsilon + 2))]}{[(q + k(\varepsilon))^2 + 1]^3 [(q - k(\varepsilon))^2 + 1]^3 [1 - \exp(-2\pi k(\varepsilon)^{-1})]}, \tag{18c}$$

$$k(\varepsilon) = (2\varepsilon - 1)^{1/2}, \tfrac{1}{2} \leqslant \varepsilon < \infty, \tag{18d}$$

with which the spectral moments, cross sections, and correlation functions of Section III can be evaluated.

A. Spectral Moments

Explicit evaluation of the sum rules of Eq. (9) provides the five analytic expressions [20, 21]

$$S(q, 2) = \tfrac{4}{3} + q^2 + \tfrac{1}{4}q^4 \tag{19a}$$

$$S(q, 1) = \tfrac{2}{3} + \tfrac{1}{2}q^2, \tag{19b}$$

$$S(q, 0) = 1, \tag{19c}$$

$$S(q, -1) = 2[1 - (1 + q^2/4)^{-4}]/q^2, \tag{19d}$$

$$S(q, -2) = \frac{(48 + 37q^2/4 + q^4 + 3q^6/64)}{12(1 + q^2/4)^5} + \frac{2\ln(1 + q^2/4)}{q^2(1 + q^2/4)^4}. \tag{19e}$$

These moments can be compared with those evaluated directly from the defining Eq. (8) using Eqs. (18). Various quadratures for the continuum contribution [23] and appropriate summation techniques for the discrete contribution [24] provide sum rules that agree with Eqs. (19) to at least ten significant figures. Gauss–Jacobi quadratures, with density parameters chosen ($\alpha = 0$, $\beta = -\frac{1}{2}$ or $\frac{3}{2}$) to insure asymptotically exact integration of the Bethe surface in the energy variable ε, and Gauss–Legendre quadratures are found to be particularly satisfactory [23]. In

connection with the summations required in the evaluation of the discrete contributions to the spectral sums, it is helpful to note (Eq. (18b)) that $f_n(q) \to f(q)/n^3$ for large n [24]. The higher order negative-integer ($k \leqslant 0$) spectral moments so obtained reproduce the known $q = 0$ values to approximately twenty significant figures [25], and, consequently, are expected to be reliable for all q values [26].

Discrete and continuum contributions to the sum rules of Eqs. (19), obtained from Eqs. (8) and (18) employing Gauss–Jacobi–Legendre quadratures and appropriate summations, are shown in Fig. 1 [27]. The discrete-spectrum contributions to $S(q, 2)$ and $S(q, 1)$ are seen to be negligibly small for $q \gtrsim 1$ a.u., indicating that these moments are dominated by the continuum portion of the spectrum [26]. Although the discrete-spectrum contributions to the other three moments are significant for small q, they evidently become negligible for $q \gtrsim 2.0$ a.u. It is found, however, that the higher order negative-integer moments $k \leqslant -3$ are dominated by the discrete spectrum for all q, and that they decrease with q according to the expression $S(q \to \infty, -k) \to (2/q^2)^k$ [28]. This decrease reflects the general shape of the Bethe surface of Eqs. (18), which includes a pronounced maximum in the continuum oscillator-strength density (Eq. (18c))—the so-called Bethe ridge—that follows approximately the curve $\varepsilon = \frac{1}{2}q^2$ in the $\varepsilon - q$ plane at high energy and momentum transfer [8]. This ridge or maximum in the continuum oscillator-strength density is a feature common to the Bethe surfaces of all atoms and molecules, and is a consequence of the validity of the free-electron binary-encounter description of inelastic scattering at high energies [8]. By contrast, at small momentum transfer, the spectral moments $S(q, k)$ approach their dipole limits, which are uniquely determined by the corresponding photoabsorption cross sections [18]. The moment of Eq. (19d) enters subsequently in the evaluation of the static and binary-encounter approximations to differential and total inelastic scattering cross sections.

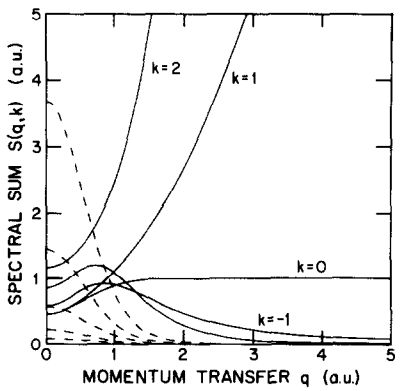

FIG. 1. Spectral sums $S(q, k)$ ($2 \geqslant k \geqslant -2$) for the Bethe surface in atomic hydrogen: (- - -) discrete and (—) continuum contributions obtained from Eqs. (8) and (18) employing Gauss–Jacobi–Legendre quadratures and appropriate summations. The discrete contributions, which are not labeled, decrease sequentially in the order $k = -2, -1, 0, 1, 2$. All values in Hartree atomic units.

B. Scattering Cross Sections

Precise evaluation of the scattering cross sections differential in momentum transfer and in scattering angle, and of the total inelastic scattering cross section, provides the basis for clarification of corresponding static, binary-encounter, and sum-rule approximations.

In the context of the scattering cross section of Eqs. (10), wherein the variables q and ε are employed, the so-called static approximation corresponds to taking the limits [4–6, 29, 30]

$$\varepsilon_{\max}(q) \to \infty \tag{20a}$$

$$S(\varepsilon_{\max}(q), q) \to \int_{\varepsilon_1}^{\infty} (1/\varepsilon)\, df(\varepsilon, q) = S(q, -1) \tag{20b}$$

in Eqs. (10) for all values of momentum transfer. Consequently, the static approximation to the scattering cross section differential in momentum transfer (Eq. (10a)) is simply

$$d^{(1)}\sigma_s(q) = (2\pi/qt)\, S(q, -1)\, dq. \tag{20c}$$

Evidently, the only approximation made in obtaining Eq. (20c) is the extension of the integration in Eq. (10b) to infinity, involving an approximation to the kinematical relation of Eq. (10c), the effects which can be readily discerned by comparison with precise evaluation of Eqs. (10). In view of Eqs. (10c) and (14b), it is anticipated that the approximation of Eqs. (20) can be a poor one for both small and large values of q at a fixed incident energy t. In the former case $\varepsilon_{\max}(q) \to \varepsilon_1$ as $q \to q_{\min}$, invalidating Eq. (20a), whereas in the latter case, the large contribution from the Bethe ridge is incorrectly included in Eq. (20b) for $q \gtrsim (2t)^{1/2}$. Because of the positive integrand involved, however, it is clear that Eq. (20c) always provides an upper bound to Eq. (10a) for all q. These observations are verified by the results shown in Fig. 2, where the $S(q, -1)$ sum rule for atomic hydrogen (Eq. (19d)) is compared with convergent values of the factor $S(\varepsilon_{\max}(q), q)$ (Eqs. (10)) for four values of incident energy. Quadrature techniques similar to those employed in evaluating spectral moments are used in determining precise values of Eq. (10b) from Eqs. (18) [26].

Evidently, the correct and static results in atomic hydrogen shown in Fig. 2 are in good agreement for all incident energies except at very small and large values of momentum transfer. The failure of the approximation at large q is apparent in the figure only for the smallest value of incident energy considered (1 keV $\cong$ 36.7 a.u.), however. Although the latter may seem to be a low incident energy, it is two orders of magnitude greater than the ionization potential in atomic hydrogen, and thus in the range of validity of the Born approximation [31]. Since the $S(q, -1)$ sum rule is in any event small in the neighborhood of $q_{\max}$ (Eq. (14b)), and in view of the $(1/q)$ factor in Eq. (20c), the discrepancy at large q is perhaps not a significant one [32]. The failure of the static approximation at small momentum transfer is always significant, however, in that no matter how high the incident energy, the $S(q, -1)$

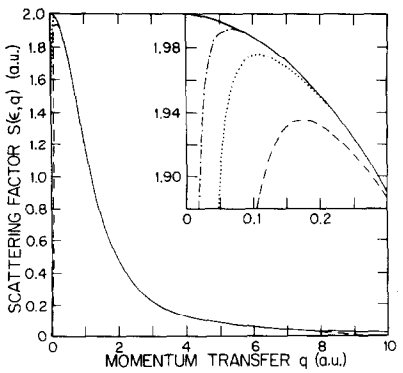

FIG. 2. Scattering factor $S(\varepsilon_{max}(q), q)$ appearing in the Bethe–Born inelastic cross section differential in momentum transfer for atomic hydrogen; convergent correct values of Eqs. (10) and (18): (- - -) $t = 1$ keV; (···) $t = 5$ keV; (- · -) $t = 25$ keV; (—) $S(q, -1)$ static approximation of Eq. (19d). Ordinate and abscissa in Hartree atomic units.

sum rule has a finite limit as $q \to q_{min}$, whereas the correct scattering factor $S(\varepsilon_{max}(q), q)$ goes to zero as $q \to q_{min}$ in every case. Consequently, the static approximation to the cross section (Eq. 20c)) is large and finite as $q \to q_{min}$, whereas the correct scattering cross section differential in momentum transfer (Eq. (10a)) has a zero limit as $q \to q_{min}$. With the exception of the large and small q regions, the results of Fig. 2 indicate that the static approximation to the inelastic cross section differential in momentum transfer is a good one in atomic hydrogen over the kinematically allowable range of momentum transfer, and provides an upper bound to the correct values.

An alternative to the static approximation (Eq. (20c)) to the cross section differential in momentum transfer (Eqs. (10)) is obtained in the spirit of the binary-encounter approximation [4–6] by replacing the correct oscillator-strength density (Eqs. (18)) in Eq. (10b) with the expression

$$g_{be}(\varepsilon, q) = N_{be}(q)\, \varepsilon[(\varepsilon - q^2/2)^2 + q^2]^{-3}, \tag{21a}$$

where the normalization factor $N_{be}(q)$ is chosen to satisfy [34]

$$S(q, -1) = N_{be}(q) \int_{\varepsilon_1}^{\infty} [(\varepsilon - q^2/2)^2 + q^2]^{-3}\, d\varepsilon. \tag{21b}$$

Equation (21a) provides an approximation to the Bethe ridge appearing in the correct oscillator-strength density of Eq. (18c) [8], and reflects the free-electron binary-encounter description of inelastic scattering at high energy. Although Eq. (21a) is appropriate specifically for atomic hydrogen, a similar sum-rule constrained approximation can be devised for arbitrary atoms and molecules provided an appropriate ionization energy is incorporated in the development [8, 34].

Introducing the approximation of Eqs. (21a) and (21b) into Eqs. (10a) and (10b) and integrating over the kinematically correct range of excitation energy $(\varepsilon_t, \varepsilon_{\max}(q))$ gives

$$d^{(1)}\sigma_{\text{be}}(q) = (2\pi/qt)\, S_{\text{be}}(\varepsilon_{\max}(q), q)\, dq, \tag{21c}$$

where

$$S_{\text{be}}(\varepsilon_{\max}(q), q) = N_{\text{be}}(q) \int_{\varepsilon_t}^{\varepsilon_{\max}(q)} [(\varepsilon - q^2/2)^2 + q^2]^{-3}\, d\varepsilon,$$

$$= (2/q^2)[1 - (1 + q^2/4)^{-4}]\, \frac{[f(k_1 - q) - f(\varepsilon_t/q - q/2)]}{[\pi/2 - f(\varepsilon_t/q - q/2)]},$$

$$q_{\min} \leqslant q \leqslant q_{\max}, \tag{21d}$$

with

$$f(x) = \tan^{-1}x + x/(x^2 + 1) + 2x/3(x^2 + 1)^2. \tag{21e}$$

The explicit prescription of Eq. (21d) restricting q values to the kinematically allowed range is required to avoid the prediction of negative values. Because the kinematically correct limits of integration are incorporated in the development of Eqs. (21), the binary-encounter approximation to the scattering factor of Eq. (10b) exhibits the correct large and small q behaviors, whereas the static approximation does not. This point is illustrated in Fig. 3, where static (Eq. (20b)), binary-encounter (Eq. (21d)),

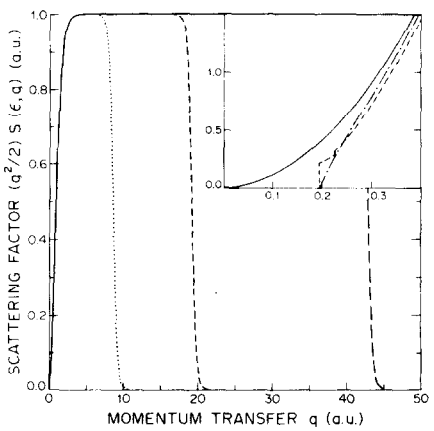

FIG. 3. Scattering factor $(q^2/2)S(\varepsilon_{\max}(q), q)$ appearing in the Bethe–Born inelastic cross section differential in momentum transfer for atomic hydrogen: (—) static approximation of Eq. (20b); other curves refer to both convergent values of Eq. (10b) and corresponding binary-encounter values of Eqs. (21d) and (21e); (···); $t = 1$ keV; (- - -), $t = 5$ keV; (– – –) $t = 25$ keV. In the small-q insert are shown the static result and the correct and binary-encounter (– · –) results for $t = 5$ keV. All values in Hartree atomic units.

and correct (Eq. (10b)) values of the scattering factor $(q^2/2)\,S(\varepsilon_{max}(q), q)$ are compared. Evidently the binary-encounter approximation of Eqs. (21a)–(21e) is indistinguishable from the correct Born values on the scale of the figure for the incident energies considered, whereas the static approximation (Figs. 2 and 3) is incorrect in both the large- and small-q limits. Moreover, as is evident from the insert in Fig. 3, the binary-encounter approximation of Eqs. (21) is in excellent agreement with the correct Born result of Eqs. (10) even in the immediate neighborhood of q_{min} (Eq. (14b)), where the contributions from the individual discrete states are discernible in the correct cross section [26].

In accordance with the discussion in Section III, it is clear that the cross section of Eq. (10a) at fixed momentum transfer does not correspond to a single scattering angle, but rather to a range of angles between $\theta_{min}(q)$ and $\theta_{max}(q)$, as given by the expressions of Eqs. (11). Consequently, although Eqs. (20) can provide a generally good approximation to the scattering cross section of Eq. (10a) at fixed momentum transfer (Figs. 2 and 3), the corresponding static approximation to the cross section differential in scattering angle (Eq. (12a)) can be poor. The static approximation to Eq. (12a) is [4–6, 29, 30]

$$d^{(1)}\sigma_s(\theta) = 4\pi F_s(\theta) \sin\theta\, d\theta, \tag{22a}$$

where

$$F_s(\theta) = S(q_e(\theta), -1)/q_e(\theta)^2. \tag{22b}$$

Equations (22a) and (22b) are obtained from Eq. (12b) by replacing the kinematically correct scattered electron momentum with its elastic-limit value ($k_2/k_1 \to 1$, all ε)—in which case the momentum transfer $q(\varepsilon, \theta)$ of Eq. (4) also takes on the elastic-limit value

$$q_e(\theta) = 2t^{1/2}(1 - \cos\theta)^{1/2} = 2(2t)^{1/2} \sin(\theta/2) \tag{22c}$$

—and extending the upper limit of the integral over excitation energy in Eq. (12b) to infinity. Consequently, the approximation inherent in Eqs. (22) is apparently distinct from that employed in Eqs. (20).

In view of the large contribution to the inelastic cross section of Eq. (12a) from the Bethe ridge, it can be expected that a useful approximation to $d^{(1)}\sigma(\theta)$ is obtained from Eq. (12b) employed the binary-encounter approximation [4–6, 33]. In this approach, the kinematically correct scattered electron momentum k_2 and associated momentum transfer $q(\theta)$ are replaced by the corresponding free-electron binary-encounter values. The former is given by the expression

$$(k_2/k_1)_{be} = (1 - \varepsilon_1/t)^{1/2} \qquad \text{for} \quad 0 \leqslant \theta \leqslant \theta_1, \tag{23a}$$

$$= (1 - q_{be}(\theta)^2/(2t))^{1/2} \qquad \text{for} \quad \theta_1 \leqslant \theta \leqslant \pi, \tag{23b}$$

and the latter by

$$q_{be}(\theta) = q(\varepsilon_1, \theta) \qquad \text{for} \quad 0 \leqslant \theta \leqslant \theta_1 \tag{24a}$$

$$= (2t)^{1/2} \sin\theta \qquad \text{for} \quad \theta_1 \leqslant \theta \leqslant \pi/2, \tag{24b}$$

$$= (2t)^{1/2} \qquad \text{for} \quad \pi/2 \leqslant \theta \leqslant \pi, \tag{24c}$$

where $q(\varepsilon_1, \theta)$ and θ_1 are given by Eqs. (13). Finally, the integral over excitation energy is extended to infinity, and the factor $F_s(\theta)$ in Eq. (22b) is consequently replaced in the binary-encounter approximation by

$$F_{be}(\theta) = S(q_{be}(\theta), -1)(k_2/k_1)_{be}/q_{be}(\theta)^2. \tag{25}$$

The ranges of validity of Eqs. (22) to (25) can be tested by comparison with the correct scattering factor $F(\theta)$. Since $F(\theta)$, $F_s(\theta)$, and $F_{be}(\theta)$ vary by many orders of magnitude in the range $0 \leqslant \theta \leqslant \pi$, however, it is convenient to note that

$$F_s(\theta) \to 2/q_e(\theta)^4, \qquad t \to \infty,$$

$$= 1/(8t^2(1 - \cos\theta)^2), \tag{26}$$

and to consider, rather, the scattering factor

$$H(\theta) = 8t^2(1 - \cos\theta)^2 F(\theta), \tag{27}$$

as well as correspondingly defined factors $H_s(\theta)$ and $H_{be}(\theta)$.

In Fig. 4, the correct scattering factor $H(\theta)$, obtained from Eqs. (12) and (18) and appropriate quadrature techniques, is compared with $H_s(\theta)$ and $H_{be}(\theta)$ obtained from

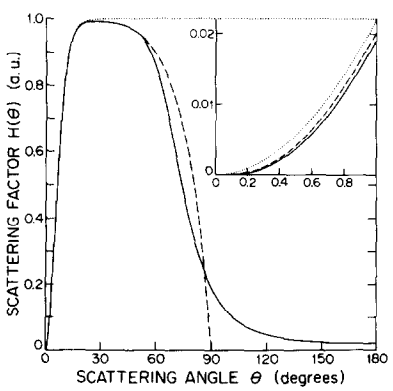

FIG. 4. Scattering factor $H(\theta)$ of Eq. (27) appearing in the Bethe–Born inelastic cross section differential in scattering angle for atomic hydrogen at $t = 1$ keV indicent energy: (—) correct values of Eqs. (12b), (18), and (27); (···) static approximation $H_s(\theta)$ of Eqs. (22) and (27); (- - -) binary-encounter approximation $H_{be}(\theta)$ of Eqs. (25) and (27). Curves qualitatively similar to those shown here are also obtained for $t = 5$ and 25 keV incident energy [26]. Ordinate in Hartree atomic units.

Eqs. (22) and (25), respectively, as functions of scattering angle θ for $t = 1$ keV incident kinetic energy. Evidently, the static approximation $H_s(\theta)$ provides a good representation of $H(\theta)$ in atomic hydrogen for scattering angles $\theta \lesssim 30°$, although an incorrect limit is approached for large θ. By contrast, the binary-encounter approximation $H_{be}(\theta)$ goes to zero for $\theta \geqslant 90°$, and provides a useful approximation for intermediate scattering angles. Although it is not apparent from the figure, $H_s(\theta)$ and $H_{be}(\theta)$ have incorrect behaviors as $\theta \to 0$, and the corresponding factor $F_s(\theta)$ diverges in this limit, whereas $F(\theta)$ is finite at $\theta = 0$. This divergence can, of course, be avoided by restricting Eqs. (22) to kinematically correct momentum-transfer values greater than or equal to the kinematically correct q_{min} of Eq. (14b). For larger incident energies t, the correct $H(\theta)$ and binary-encounter $H_{be}(\theta)$ scattering factors are of the same general form as shown in Fig. 4 and are in increasingly good agreement with increasing t, whereas the static result $H_s(\theta)$ continues to provide an incorrect limit ($H_s(\theta) \to 1$) for large scattering angle [26].

Finally, approximations to the total inelastic scattering cross section of Eqs. (14) and (15) are investigated. The static approximation in this case is obtained from Eqs. (14) and (20) in the form [35, 36]

$$\sigma_{static} = (2\pi/t) \int_{q_{min}}^{q_{max}} (1/q)\, S(q, -1)\, dq. \tag{28}$$

Making use of Eq. (19d), the integral of Eq. (28) takes the form

$$\sigma_{static} = (2\pi/t)[\ln(x/(1+x)) + (9x^2 + 21x + 13)/12(1+x)^3]_{x=q_{min}^2/4}^{x=q_{max}^2/4}. \tag{29}$$

An excellent approximation to Eq. (29) is obtained from the leading terms in $(1/t)$ and $\ln(t)/t$ in the form ($\varepsilon_1 = 0.375$ a.u.)

$$(t/2\pi)\sigma_{static} \to \ln(t) + \ln(8/\varepsilon_1^2) - \tfrac{13}{12} = \ln(t) + 2.96. \tag{30}$$

A binary-encounter approximation to the total inelastic scattering cross section is obtained from Eqs. (14) and (21) in the form

$$\sigma_{be} = (2\pi/t) \int_{q_{min}}^{q_{max}} (1/q)\, S_{be}(\varepsilon_{max}(q), q)\, dq. \tag{31}$$

Although the integral of Eq. (31) cannot be evaluated in closed analytic form, extraction of the leading terms gives the convenient asymptotic ($t \to \infty$) expression [37]

$$(t/2\pi)\sigma_{be} \to \ln(t) + \ln(8/\varepsilon_1^2) - 89/60 = \ln(t) + 2.56 \tag{32}$$

which is seen to provide values below the static result of Eq. (30).

It is of considerable interest to note that an effective lower limit of integration q_m can always be chosen so that the correct total Born inelastic scattering cross section

(Eq. (14a)) is obtained from the static approximation of Eq. (28). The necessary condition to be satisfied is seen from Fig. 2 to be

$$(2\pi/t)\int_{q_m}^{q_1}(1/q)\,S(q,-1)\,dq + (2\pi/t)\int_{q_2}^{q_{\max}}(1/q)\,S(q,-1)\,dq$$
$$= (2\pi/t)\int_{q_{\min}}^{q_1}(1/q)\,S(\varepsilon_{\max}(q),q)\,dq + (2\pi/t)\int_{q_2}^{q_{\max}}(1/q)\,S(\varepsilon_{\max}(q),q)\,dq \quad (33)$$

where q_1 to q_2 defines the q interval over which $S(q,-1)$ and $S(\varepsilon_{\max}(q),q)$ coincide to a specified accuracy for given t (see Fig. 2). Although it is not generally possible to determine q_m from Eq. (33), its value can be inferred in the limit $t\to\infty$. In this limit $q_2 \simeq \frac{1}{2}q_{\max}\to\infty$, causing the second and fourth integrals to vanish, while q may be replaced by zero in $S(q,-1)$ and $df(\varepsilon,q)$ in the remaining integrands (Eq. (10b)). Interchanging the orders of the ε (Eq. (10b)) and q integrations in Eq. (33), writing $q_{\min}(\varepsilon)=\varepsilon/(2t)^{1/2}$ and $q_m=\varepsilon_m/(2t)^{1/2}$ in accordance with Eq. (14b), with ε_m a mean excitation energy replacing ε_1, and letting $\varepsilon_{\max}(q)\to\infty$ gives

$$S(0,-1)\int_{\varepsilon_m/(2t)^{1/2}}^{q_1}(1/q)\,dq = \int_{\varepsilon_1}^{\infty}(1/\varepsilon)\,df(\varepsilon,0)\int_{\varepsilon/(2t)^{1/2}}^{q_1}(1/q)\,dq. \quad (34a)$$

Integration of this equation gives

$$S(-1)\ln\varepsilon_m = \int_{\varepsilon_1}^{\infty}(\ln(\varepsilon)/\varepsilon)\,df(\varepsilon,0) \equiv L(-1), \quad (34b)$$

where $S(0.-1)\equiv S(-1)$ and $L(-1)$ are well-known dipole sum rules [18, 38, 39]. Consequently, use of the mean excitation energy

$$\varepsilon_m = \exp[L(-1)/S(-1)] \quad (35)$$

will ensure that the asymptotically correct high-energy limit of the Born inelastic scattering cross section is obtained from Eq. (28) with $q_{\min}\to q_m=\varepsilon_m/(2t)^{1/2}$. In the particular case of atomic hydrogen, Eq. (29) with $\varepsilon_1\to\varepsilon_m$ gives ($\varepsilon_m=0.465$ a.u. [38, 39])

$$(t/2\pi)\sigma_{\text{inelastic}} \to \ln(t) + \ln(8/\varepsilon_m^2) - 13/12. \quad (36a)$$

Moreover, retaining the next higher order term in the development of Eqs. (33) – (35) gives

$$(t/2\pi)\sigma_{\text{inelastic}} \to \ln(t) + \ln(8/\varepsilon_m^2) - 13/12 - (7/8)/t$$
$$= \ln(t) + 2.53 - (7/8)/t. \quad (36b)$$

The results of Eqs. (33)–(36) are seen to be identical with the so-called Bethe–Inokuti

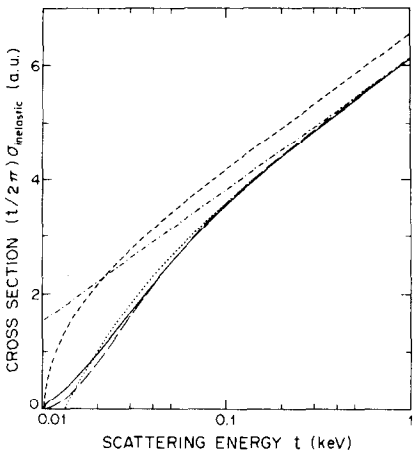

FIG. 5. Fano plot of the total Bethe–Born inelastic scattering cross section in atomic hydrogen: (—) correct values of Eqs. (14) and (18); (– · –) sum-rule approximation of Eq. (36a); (···) sum-rule approximation of Eq. (36b); (- - -), static approximation of Eq. (29); (– – –), binary-encounter approximation of Eq. (31). All values in Hartree atomic units except as indicated.

asymptotic approximation to the total inelastic scattering cross section [8, 35], derived earlier employing the correct asymptotic expressions for individual-state excitation cross sections and subsequent summations [38].

In Fig. 5, the predictions of Eqs. (28)–(36) are compared with the correct total Born inelastic scattering cross section of Eqs. (14) and (18), obtained by employing appropriate quadratures [23, 40]. Evidently, the asymptotically correct cross section of Eq. (36b) is a very good approximation to the correct Born result over the entire range of allowable scattering energies, with the error never exceeding 5% in the energy range $t \gtrsim 50$ eV. Of course, it should be recognized that the Born cross section itself is no longer satisfactory for scattering energies below ~50 eV in this case. The binary-encounter approximation of Eq. (32) is also in good accord with the Born cross section for all incident energy. By contrast, the static approximation of Eq. (29) is seen to be generally less satisfactory, even in the high-energy limit. These results suggest that the simple binary-encounter expression of Eqs. (21) and (31) can be highly satisfactory, and that the $S(q, -1)$ sum rule is sufficient for determinations of accurate approximations to total inelastic scattering cross sections provided an appropriate (Eqs. (33)–(36)) lower limit is employed in the integration over momentum transfer.

C. *Van Hove Correlation Functions*

Discrete and continuum contributions to the real and imaginary parts of the correlation functions of Eqs. (16) in atomic hydrogen are evaluated employing Eqs. (18) and appropriate summation and quadrature techniques [26]. The results so obtained for the real parts of the autocorrelation functions for six values of

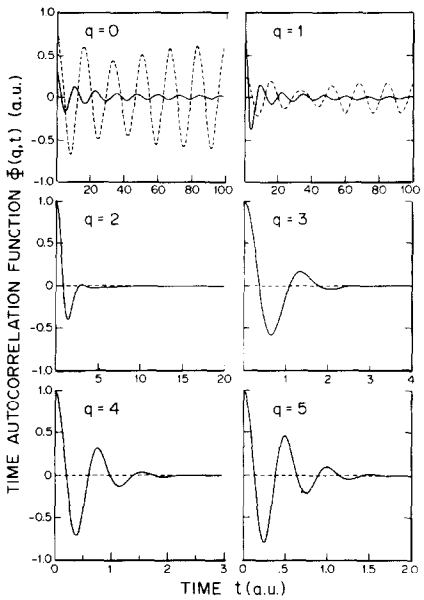

FIG. 6. Real parts of time autocorrelation functions $\Phi(q, t)$ [Eqs. (16)] in atomic hydrogen, normalized to total values at $t = 0$ by dividing by the factor $q^2 S(q, -1)/2$; (—) continuum contribution; (- - -) discrete contribution. Note the changes in time scales in the various frames. Generally similar results are obtained for the imaginary portions of Eqs. (16) (not shown). All values in Hartree atomic units.

momentum transfer are shown in Fig. 6. In each case, the total functions are normalized to unity at $t = 0$ by dividing Eq. (16a) by the value $q^2 S(q, -1)/2$. The imaginary parts (not shown) of the functions are generally similar to the results of Fig. 6 [26]. Evidently, the continuum contributions dominate the time autocorrelation functions for all q values except $q = 0, 1$, and the correlations of large-q (small wavelength) fluctuations exhibit relatively rapid decay. By contrast, the $q = 0$, or dipole time autocorrelation function in atomic hydrogen exhibits long-time oscillations, with the $q = 1$ function also showing significant oscillation. Evaluation of the autocorrelation functions for longer times in these cases indicates continuing oscillations beyond $t = 200$ a.u. (not shown) [26]. As noted by Van Hove [14], the singularities in the associated density function determine the asymptotic behavior of the time autocorrelation function. In the cases $q = 0$ and 1 it is the discrete resonance transition at ε_1 that carries the largest f number and, consequently, controls the long-time behavior of $\Phi(q, t)$. Since the Fourier transform of a delta function (Eq. (2)) is oscillatory, the results of Fig. 6 are in accord with expectation in these cases. Moreover, the secondary or envelope oscillations also evident in the cases $q = 0$ and 1 can be attributed to a beat frequency arising from interference between the $n = 2$ and 3 contributions to the discrete spectrum (Eqs. (18a) and (18b)). The $f_n(q)$ of Eq. (18b) decrease rapidly with increasing q, however, resulting in autocorrelation functions for $q = 2$–5 that have oscillatory long-time behaviors that are too small to

be seen on the scale of Fig. 6. Since the Bethe surface as a function of ε has a prominent maximum—the Bethe ridge indicated above—which broadens and extends to higher energy with increasing q, the autocorrelation functions are sharply peaked at the time origin of Fig. 6 and exhibit damped oscillations, with periods determined by the energy of the maximum of the Bethe ridge at the appropriate q_{br} value $[\tau \simeq 2\pi/\varepsilon_{br} \simeq (4\pi/q_{br}^2)]$.

The autocorrelation functions of Eqs. (16) and (17) provide an alternative perspective for study of inelastic electron-atom or -molecule scattering, in which connection approximation techniques for direct determinations of $\Phi(q, t)$ are of considerable interest [41]. Because of the absence of a useful short-time expansion of the autocorrelation function in this case, indicated in Section III(C), there is no obvious extension of the static approximation to finite time [14]. As might be expected, however, the binary-encounter approximation of Eq. (21) provides reliable autocorrelation functions for higher momentum transfer values (not shown), since it closely reproduces the Bethe ridge in atomic hydrogen. More generally, however, it will be necessary in any approximation scheme to obtain a highly reliable implicit description of the corresponding Bethe surface, since the autocorrelation function of Eqs. (16) and (17) is a rather sensitive transform of the shape of the energy-loss spectrum at a given momentum transfer. This sensitivity is in contrast to many other autocorrelation functions, which are often highly damped, and are largely insensitive to the detailed shape of the corresponding spectral function [22].

V. Concluding Remarks

In the present article, computational studies are reported of aspects of the Bethe–Born approximation to the inelastic scattering of high-energy charged particles by atoms and molecules. The relevant scattering cross sections and closely related Van Hove autocorrelation functions are identified as spectral (Riemann–Stieltjes) integral properties of the corresponding atomic and molecular Bethe surfaces. Evaluation of these properties for hydrogenic targets provides a basis for clarifying the ranges of validity of the static, binary-encounter, and sum-rule approximations to differential and total inelastic cross sections generally employed in lieu of the correct Born results. The studies are also a necessary preliminary to formulation of alternatives to conventional Bethe–Born calculations using discrete and continuum target eigenfunctions.

The static approximation to the Born inelastic cross section differential in momentum transfer is found to be generally satisfactory for sufficiently high incident energy, although incorrect results are obtained in both the low and high momentum transfer limits. By contrast, a sum-rule constrained binary-encounter approximation to the cross section differential in momentum transfer, that has received relatively little attention in the literature, is seen to provide highly accurate values at all kinematically correct momentum transfer. The static approximation to the Born inelastic cross section differential in scattering angle is also generally unsatisfactory

in the limits of both small and large scattering angles, whereas more useful results are obtained from the customary binary-encounter approximation. The Bethe–Inokuti sum-rule approximation to the total Born inelastic cross section is seen to follow directly from the static approximation and an appropriate choice of lower limit for the allowable momentum transfer integration interval. Comparison with the correct Born results indicates the approximation so obtained is highly reliable for virtually all incident energies, whereas use of the kinematically correct lower momentum transfer limit in the static approximation results in a significant overestimate of the total Born inelastic scattering cross section for all incident energies. The sum-rule constrained binary-encounter approximation to the total inelastic scattering cross section is also found to be in excellent agreement with the correct Born results. Finally, Van Hove autocorrelation functions describing target-electron charge-density fluctuations of specific wavelengths are seen to be sensitive functions of the shape of the corresponding energy-loss spectrum, suggesting they can provide a useful alternative perspective for studies of first-Born sattering cross sections. In a subsequent companion article, generalized Gaussian quadratures defined by spectral moments are employed in studies of Bethe surfaces and corresponding Van Hove autocorrelation functions [42].

ACKNOWLEDGMENTS

Acknowledgment is made to donors of the Petroleum Research Fund, administrated by the American Chemical Society, and to the National Science Foundarion for partial support of this work. It is a pleasure to thank W. P. Reinhardt and the JILA Fellows, and S. R. Langhoff, R. Jaffe, and J. O. Arnold, NASA Ames Research Center, for their kind hospitality and support of P. W. L. during early stages of the work, to thank W. J. Meath for his kind hopitality to D. J. M., to acknowledge the computational assistance of C. T. Corcoran and S. L. Seidman, and to thank R. A. Bonham for helpful comments.

REFERENCES

1. W. WHALING, *in* "Handbuch der Physik" (S. Flügge, Ed.), Vol. 34, pp. 193–217, Springer-Verlag Berlin, 1958.
2. "Studies in the Penetration of Charged Particles in Matter," National Academy of Sciences Publication 1133, Nuclear Sciences Series, Report No. 39, NAS-NRC, Washington, D. C., 1964.
3. H. BICHSEL, *in* "American Institute of Physics Handbook," 3rd ed. (D. E. Gray, Ed.), Chap. 8d, McGraw–Hill, New York, 1972.
4. R. A. BONHAM AND M. FINK, "High-Energy Electron Scattering," Van Nostrand–Reinhold, New York, 1974.
5. R. A. BONHAM, J. S. LEE, R. KENNERLY, AND W. ST. JOHN, *Adv. Quantum Chem.* **11** (1978), 1.
6. R. A. BONHAM, *in* "Electron Spectroscopy" (C. R. Brundle and A. D. Baker, Eds.), Vol. III, Academic Press, New York, 1979.
7. H. S. W. MASSEY, *in* "Handbuch der Physik" (S. Flügge, Ed.), Vol. 36, pp. 307–408, Springer-Verlag, Berlin, 1956.
8. M. INOKUTI, *Rev. Mod. Phys.* **43** (1971), 297; M. INOKUTI, Y. ITIKAWA, AND J. E. TURNER, **50** (1978), 23.

9. K. L. BELL AND A. E. KINGSTON, *Adv. At. Mol. Phys.* **10** (1974), 53; *in* "Atomic Processes and Applications" (P. G. Burke and B. L. Moiseiwitsch, Eds.), North-Holland, Amsterdam, 1976.
10. R. K. PETERKOP, "Theory of Ionization of Atoms by Electron Impact," Colorado Associated Univ. Press, Boulder, 1977, translated by D. G. Hummer.
11. H. A. BETHE, *Ann. Phys. (Leipzig)* **5** (1930), 325.
12. G. PEACH, *Proc. Phys. Soc. London* **85** (1965), 709; **87** (1966), 375; *J. Phys.* **B1** (1968), 1088; AND E. J. MCGUIRE, *Phys. Rev.* **A3** (1971), 267; **A22** (1980), 868. These journals contain extensive atomic generalized oscillator-strength calculations in the Coulomb and local-exchange approximations, respectively. Highly reliable Born calculations can be performed for discrete transitions in small atoms; B. VAN ZYL, G. H. DUNN, G. CHAMBERLAIN, AND D. W. O. HEDDLE, *Phys. Rev.* **A22** (1980), 1916; AND A. N. TRIPATHI, *Phys. Rev.* **A23** (1981), 1801. Contained herein are recent comparisons between Born theory and experiment in the case of atomic He and Li, respectively. With the exception of studies in the cases of H_2^+ and H_2 by J. M. PEEK, *Phys. Rev.* **134** (1964), A877; **139** (1965), A1429; **140** (1965), A11; **154** (1967), 52; **183** (1969), 193; and K. J. MILLER AND M. KRAUSS, *J. Chem. Phys.* **47** (1967), 3754, respectively, theoretical investigations of molecular generalized oscillator strengths are apparently limited to the discrete portion of the spectrum. S. P. KHARE AND B. L. MOISEIWITSCH, *Proc. Phys. Soc. London* **88** (1966), 605; S. P. KHARE, *Phys. Rev.* **157** (1967) 107; D. C. CARTWRIGHT, *Phys. Rev.* **A2** (1970), 1331; **5** (1972), 1974; S. CHUNG AND C. C. LIN, *Phys. Rev.* **A6** (1972), 988; **9** (1974), 1954; **17** (1978), 1874; C. W. MCCURDY AND B. V. MCKOY, *J. Chem. Phys.* **61** (1974), 2820; S. CHUNG, C. C. LIN, AND E. T. P. LEE, *Phys. Rev.* **A12** (1975), 1340; T. N. RESCIGNO, C. F. BENDER, AND B. V. MCKOY, *Chem. Phys. Lett.* **45** (1977), 307. The impact-parameter method of M. J. SEATON, *Proc. Phys. Soc. London* **79** (1962), 1105, recently refined and applied by A. U. HAZI, *Phys. Rev.* **A23** (1981), 2232. in the case of discrete molecular excitations should also be applicable to studies of molecular ionization, although applications are apparently not available at present. Theoretical and semiempirical methods for accurate determinations of atomic and molecular stopping, straggling, and excitation energies that avoid explicit construction of the generalized oscillator-strength distribution are described by P. W. LANGHOFF AND A. C. YATES, *J. Phys.* **B5** (1972), 1071, and G. D. ZEISS, W. J. MEATH, J. C. F. MACDONALD, AND D. J. DAWSON, *Radiat. Res.* **70** (1977), 284.
13. P. W. LANGHOFF, *Int. J. Quantum Chem.* **S8** (1974), 347; P. W. LANGHOFF AND S. L. SEIDMAN, *Chem. Phys. Lett.* **27** (1974), 195.
14. L. VAN HOVE, *Phys. Rev.* **95** (1954), 249.
15. Corrections for the effects of electron exchange not included in Eq. (1) are discussed by H. S. W. MASSEY AND C. B. O. MOHR, *Proc. R. Soc. London Ser. A* **A132** (1931), 605; S. KHASHABA AND H. S. W. MASSEY, *Proc. Phys. Soc. London* **71** (1958), 574; and more recently by R. A. BONHAM, *J. Chem. Phys.* **36** (1962), 3260, and R. A. BONHAM AND C. TAVARD, *J. Chem. Phys.* **59** (1973), 4691. It is perhaps also appropriate to note here that improvements and refinements of Eq. (1) have been suggested by Y. HAHN, *Phys. Lett.* **62A** (1977), 310, and that a Born–Møller generalization of Eq. (1) applicable in the MeV range has been employed recently in K-shell impact-ionization cross section calculations by J. TSERKRISME NDEFRU, J. G. WILLS, AND F. B. MALIK, *Phys. Rev.* **A21** (1980), 1049.
16. H. A. BETHE AND E. E. SALPETER, "Quantum Mechanics of One- and Two-Electron Atoms," Academic Press, New York, 1957.
17. J. A. SHOHAT AND J. D. TAMARKIN, "The Problem of Moments," Mathematical Surveys **1**, American Mathematical Society, Providence, 1950.
18. P. W. LANGHOFF, *J. Chem. Phys.* **57** (1972), 2604.
19. P. W. LANGHOFF, *in* "Electron-Molecule and Photon-Molecule Collisions" (T. N. Rescigno, B. V. McKoy, and B. Schneider, Eds.), pp. 183–224, Plenum, New York/London, 1979; and *in* "Theory and Applications of Moment Methods in Many-Fermion Systems" (B. J. Dalton, S. M. Grimes, J. P. Vary, and S. A. Williams, Eds.), pp. 191–212, Plenum, New York, 1980.
20. J. O. HIRSCHFELDER, W. B. BROWN, AND S. T. EPSTEIN, *Adv. Quantum Chem.* **1** (1964), 255; R. JACKIW, *Phys. Rev.* **157** (1967), 1220.

21. G. LAMM AND A. SZABO, *J. Phys.* **B10** (1977), 1967.
22. W. MARSHALL AND S. W. LOVESEY, "Theory of Thermal Neutron Scattering," Oxford Univ. Press. Oxford, 1971; D. A. MCQUARRIE, "Statistical Mechanics," Harper and Row, New York, 1976; B. J. BERNE (Ed.) *in* "Modern Theoretical Chemistry," Plenum, New York, 1977.
23. P. J. DAVIS AND I. POLONSKY, *in* "Handbook of Mathematical Functions" (M. Abramowitz and I. A. Stegan, Eds.), Dover, New York, 1965.
24. J. M. HARRIMAN, *Phys. Rev.* **101** (1956), 594; M. INOKUTI, Argonne National Laboratory Report No. ANL-6769, 1963.
25. R. J. BELL, *Proc. Phys. Soc. London* **92** (1967), 842; P. W. LANGHOFF AND M. KARPLUS, *J. Chem. Phys.* **52** (1970), 1435.
26. Additional theoretical and computational details are given separately by D. J. MARGOLIASH, Ph. D. dissertation, Indiana University, Bloomington, 1980, unpublished.
27. Discrete and continuum contributions to $S(q,-1)$ of Eq. (19d) have been reported previously by G. H. GILLESPIE, *Phys. Rev.* **A18** (1978), 1967.
28. H. F. WELLENSTEIN, R. A. BONHAM, AND R. C. ULSH, *Phys. Rev.* **A8** (1974), 304.
29. P. M. MORSE, *Phys. Z.* **33** (1932), 443.
30. R. A. BONHAM, *Chem. Phys. Letters* **18** (1973), 454.
31. L. I. SCHIFF, "Quantum Mechanics," pp. 324–326, McGraw–Hill, New York, 1968.
32. A somewhat more detailed analysis of the static approximation of Eqs. (20) indicates that better than 1% accuracy is obtained from Eq. (20c) in the large q region for $q \lesssim k_1 - 1.5$ a.u. [26].
33. R. A. BONHAM, *Chem. Phys. Lett.* **52** (1977), 305.
34. For an alternative recent discussion of sum-rule constrained binary-encounter approximations, see C. J. TUNG, *Phys. Rev.* **A22** (1980), 2550.
35. M. INOKUTI, Y.-K. KIM, AND R. L. PLATZMAN, *Phys. Rev.* **164** (1967), 55.
36. R. A. BONHAM AND E. W. NG, *Chem. Phys. Lett.* **4** (1969), 355; **6** (1970), 403.
37. Extraction of the leading terms from Eq. (31) is accomplished by appropriate expansion of the function $f(x)$ of Eq. (21e) prior to performing the integration over q [26].
38. W. F. MILLER AND R L. PLATZMAN, *Proc. Phys. Soc. London* **70** (1957), 299; Y.-K. KIM AND M. INOKUTI, *Phys. Rev.* **A3** (1971), 665.
39. P. W. LANGHOFF AND A. C. YATES, *Phys. Rev. Lett.* **25** (1970), 1317.
40. L. VRIENS AND T. F. M. BONSEN, *J. Phys.* **B1** (1968), 1123.
41. B. SCHNEIDER, *Phys. Rev.* **A2** (1970), 1873.
42. D. J. MARGOLIASH AND P. W. LANGHOFF, *J. Comput. Phys.* **49** (1983), 67.